Surface characteristics, collector adsorption, and flotation response of covellite in oxidizing environment

Yong-gang GAN[1,2,3], Rong-dong DENG[4], Quan-jun LIU[1]

1. Faculty of Land Resource Engineering, Kunming University of Science and Technology, Kunming 650093, China;
2. Serbia Zijin Mining Doo Bor, Bor 19210, Serbia;
3. Zijin Mining Group Co., Ltd., Longyan 364200, China;
4. School of Zijin Mining, Fuzhou University, Fuzhou 350108, China

Abstract: The surface characteristics, collector adsorption, and flotation response of covellite in the presence of NaClO and $FeCl_3$ were investigated using micro-flotation tests, X-ray photoelectron spectroscopy (XPS), time-of-flight secondary ion mass spectrometry (TOF-SIMS), and contact angle measurements. The micro-flotation test results indicated that covellite was effectively inhibited by the presence of NaClO and $FeCl_3$. However, the dosages of these depressants were large, and the conditioning time was long. The results of the XPS and TOF-SIMS analyses indicated that NaClO could oxidize the covellite surface and reduce the active sites of Cu. Oxidation products, including CuO and $Cu(OH)_2$, were generated on the covellite surface. After the addition of $FeCl_3$, the precipitation of iron hydroxide on the covellite surface increased the content of hydrophilic species on the mineral surface. Thus, the adsorption of ammonium dibutyl dithiophosphate on covellite surface was prevented, which reduced the floatability of the covellite.
Key words: covellite; floatability; TOF-SIMS; NaClO; $FeCl_3$

1 Introduction

Covellite (CuS) is an important copper-bearing mineral because of its high value as a commercial source of copper [1]. It is a secondary copper sulfide and is associated with the alteration of other copper sulfides, such as chalcocite, digenite, and bornite [2,3]. Flotation is the main method used to concentrate covellite, which has good floatability. In this process, covellite attaches to the air bubbles and is transported into the froth phase for recovery, leaving the gangue in the tailing [4,5].

However, covellite is always associated with enargite in copper mines [6]. Arsenic, which is a constituent element of enargite, is a harmful element in copper concentrates. Many countries require smelters to maintain the arsenic levels in copper concentrates at or below 0.2 wt.% [7,8]. To meet these arsenic level requirements for copper concentrates, covellite and enargite need to be separated. In the process of separating covellite and enargite by flotation, the floatability of the covellite needs to be suppressed. Oxidation is the main method used to inhibit the floatability of covellite. In a strong oxidizing environment, the surface of the covellite becomes hydrophilic, while good floatability of the enargite is maintained. However, this is not easy because covellite and enargite are both copper-bearing minerals and have similar flotation properties [9,10].

Numerous previous studies have investigated methods for separating enargite and copper sulfide minerals (chalcocite, covellite, chalcopyrite,

bornite, and tennantite) during the flotation stage of mineral processing operations [11−13]. Electrochemical oxidation, hydrogen peroxide, hypochlorite, and potassium permanganate have been used to oxidize copper sulfide minerals and achieve separation [14]. However, to date, no effective flotation method capable of selectively targeting arsenic minerals in industrial applications has been developed [15]. Although great progress has been made in understanding the flotation response of enargite, the effect of oxidation on the surface properties of covellite in the flotation process remains unclear. A fundamental understanding of covellite surface chemistry must be obtained before fully implementing mechanisms for successful separation by flotation.

This study investigated the oxidation characteristics of covellite, along with its wettability, surface element changes, collector adsorption behavior, and flotation behavior under oxidation conditions. The aim of this study was to determine the change law and related mechanism of covellite floatability in an oxidizing environment.

2 Experimental

2.1 Materials and reagents

High-purity samples of natural covellite were handpicked from the Timok Mine (Serbia). Initially, these samples were washed with distilled water and dried. Subsequently, the samples were processed in a porcelain ball mill, sieved, and classified to obtain the desired particle size fractions. Mineralogical and chemical analyses and X-ray diffraction (XRD) spectra indicated that the purity of these covellite particles exceeded 93%. The results of the XRD analysis are shown in Fig. 1.
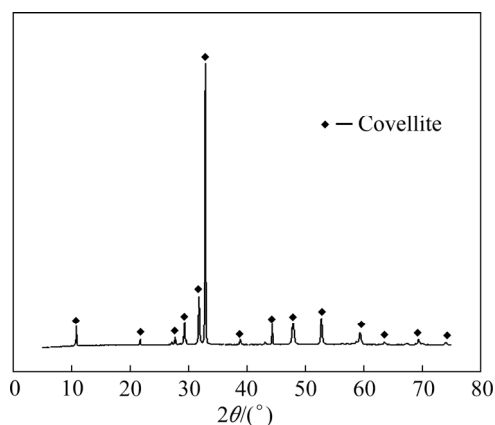

Fig. 1 XRD pattern of covellite

The reagents used in this study are listed in Table 1. Deionized water was used throughout the experiments, which were conducted at (26 ± 1) °C.

Table 1 Reagents used in experiments

Chemical	Content/wt.%	Supplier	Role
HCl	36	Sinopharm Chemical	pH adjuster
NaOH	98	Sinopharm Chemical	pH adjuster
FeCl$_3$	98	Sinopharm Chemical	Depressant
NaClO	8	Sinopharm Chemical	Depressant
Ammonium dibutyl dithiophosphate	–	Penn Chemical	Collector
MIBC	99	Penn Chemical	Frother

2.2 Methods

2.2.1 Micro-flotation

Pure covellite was ground using an agate mortar and pestled and dry-screened to obtain the desired particle size fractions (38−74 μm) before the flotation tests. The micro-flotation experiments were conducted in a mechanical agitation flotation machine with a rotational speed of 1992 r/min. In each test, 3 g of the mineral sample was placed in a flotation cell with 30 mL of deionized water. Firstly, dilute HCl and NaOH solutions were used to regulate the pH of the pulp solution. After 1 min of agitation, freshly prepared NaClO and FeCl$_3$ solutions of the desired concentrations were sequentially added with certain conditioning time. Subsequently, the ammonium dibutyl dithiophosphate (ADD, 1×10^{-5} mol/L) collector and methyl isobutyl carbinol (MIBC, 1×10^{-5} mol/L) frother were sequentially added, and their conditioning time was 2 and 1 min, respectively. Finally, the flotation was performed for 5 min. The concentrate products obtained from the flotation were collected, filtered, weighed, and dried. The flotation recovery was then calculated based on the solid mass.

2.2.2 XPS measurements

The covellite samples treated with different reagents were analyzed using X-ray photoelectron spectroscopy (XPS) (ESCALAB 250, VG Systems, UK). The sample used for the XPS measurement

was obtained by adding 0.5 g of covellite powder (38−74 μm) to the slurry solution (50 mL) at pH 10. The mineral suspension was first conditioned with a 2000 mg/L NaClO stock solution and stirred for 30 min. The $FeCl_3$ solution was then poured into the slurry solution until the iron ion concentration of the solution reached 500 mg/L. The mixture was magnetically stirred for another 10 min. After treatment with the reagents, the supernatant was removed via the siphon method, and then washed, filtered, and vacuum dried at 40 °C.

A survey scan of the analyzed sample was initially conducted to detect the elemental substances, and a precise scan was then performed to obtain the XPS spectrum of each specific element. Avantage software (Thermo Scientific, UK) was used to analyze the XPS data, including peak fitting and semiquantitative estimation. The C 1s spectral peak (284.8 eV) was obtained to calibrate all the measured spectra as an internal standard for charge compensation.

2.2.3 Contact angle measurements

The contact angles of the covellite samples were measured with a DSA255 goniometer (DSA25S, KRŰSS, Germany) using the sessile drop method. A slicer was used to cut the pure covellite samples into pieces of approximately 10 mm × 10 mm × 5 mm, and the samples were sequentially polished with 400, 600, and 1200 grit silicon carbide sandpaper in sequence. Then, hydrochloric acid and ultrapure water were used to clean the polished samples several times, followed by drying the samples under vacuum. Agents were added to the treated samples using the same processing method as for the flotation tests, and the surfaces of the samples were cleaned with ultrapure water and dried under vacuum at 40 °C. After conditioning, each sample was placed on the stage of the contact angle measuring instrument with its polished surface upward, and a 3.0 μL ultrapure water droplet (18 MΩ·cm) was dropped on the polished surface of the sample. Next, the contact angles of the samples were simultaneously measured using the ADVANCE software (KRŰSS, Germany), which automatically calculated the data based on the contour of the droplets on the surface. Each sample was measured three times to obtain an average and ensure the accuracy of the experimental results.

2.2.4 TOF-SIMS measurements

The properties of the covellite surface were characterized using time-of-flight secondary ion mass spectrometry (TOF-SIMS) analysis (ION-TOF, Munster, Germany). The covellite samples were prepared using the same method used for contact angle measurements. The typical measurement conditions for the surface analysis included a primary ion source of Bi_3^+, a primary ion energy of 15 keV, a current of 0.45 pA, an area of 100 μm × 100 μm, and a measurement time of 237 s. All the samples were placed in the middle of an electron gun, and the vacuum degree was $1×10^{-7}$ Pa, at least during the time of analysis.

3 Results and discussion

3.1 Micro-flotation

3.1.1 Effect of pH on flotation performance of covellite

Single mineral flotation tests with ADD as the collector, NaClO and $FeCl_3$ as the depressants, and MIBC as the frother were conducted to observe the effects of different conditions on the flotation performance of covellite. NaClO is a strong oxidant that can oxidize the surface of sulfide minerals. By contrast, $FeCl_3$ is weaker in oxidation, but it can promote iron hydroxide precipitation and cover the surface of minerals, thereby inhibiting them [16].

The flotation performance of covellite as a function of pH is shown in Fig. 2. The results indicated that covellite had high floatability in the
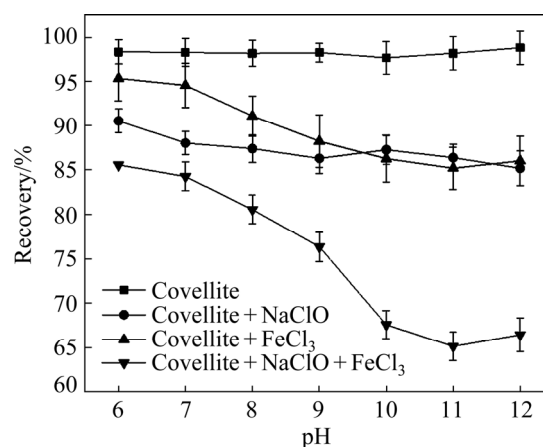

Fig. 2 Effect of pH on flotation performance of covellite (c(ADD)=1×10^{-5} mol/L; c(NaClO)=2000 mg/L; c($FeCl_3$)=2000 mg/L; c(NaClO+$FeCl_3$)=(1500+500) mg/L; conditioning time of NaClO and $FeCl_3$ 10 and 5 min, respectively)

tested pH range in the absence of a depressant. More than 98% of the covellite was recovered between pH 6 and 12, indicating that the floatability of natural covellite was not affected by the pH. In the presence of NaClO or $FeCl_3$ alone, the floatability of the covellite gradually decreased with the increasing pH. When NaClO and $FeCl_3$ were used as depressants to inhibit the covellite, the mineral floatability was greatly affected by the pH, with an alkaline environment increasing the inhibitory effect on the covellite particles. In addition, it was clearly found that it was difficult to inhibit covellite, and the effect of two agents at the same time was much better.

3.1.2 Effect of mass ratio of NaClO to $FeCl_3$ on flotation performance of covellite

When two agents were used simultaneously, their mass ratio affected the floatability of the mineral [17]. The effects of the mass ratio of NaClO to $FeCl_3$ on covellite flotation were examined, and the results are shown in Fig. 3. As shown in Fig. 3, the proportion of $FeCl_3$ in the depressant mixture affected the floatability of the covellite. As the mass ratio of NaClO to $FeCl_3$ increased from 1:1 to 4:1, the recovery of covellite decreased from 74.2% to a minimum of 63.67%. A higher mixture ratio resulted in a better depression effect. The ideal separation result was obtained with an optimum mass ratio of NaClO to $FeCl_3$ being 4:1.
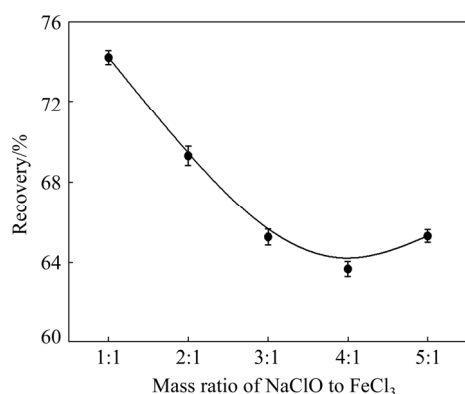

Fig. 3 Effect of mass ratio of NaClO to $FeCl_3$ on flotation of covellite (c(ADD)=1×10^{-5} mol/L; c(NaClO+$FeCl_3$)=2000 mg/L; conditioning time of NaClO and $FeCl_3$ 10 and 5 min, respectively; pH=10)

3.1.3 Effect of depressant dosage on flotation of covellite

The effect of the depressant dosage on the

flotation of covellite with ADD as the collector at pH 10 is presented in Fig. 4. The covellite recovery did not change significantly when the depressant dosage was below 1000 mg/L. However, when the dosage was increased, the floatability of the covellite decreased rapidly. When the dosage of NaClO and $FeCl_3$ reached 3000 mg/L, 38% of the covellite remained floating, indicating that the covellite was not easily inhibited. Therefore, the optimum dosages of NaClO and $FeCl_3$ were 2000 and 500 mg/L, respectively.

3.1.4 Effects of conditioning time of depressants on flotation of covellite

A sufficient conditioning time is necessary for the inhibition of minerals [18]. The effects of the conditioning time of NaClO and $FeCl_3$ on the flotation of covellite are presented in Fig. 5. The
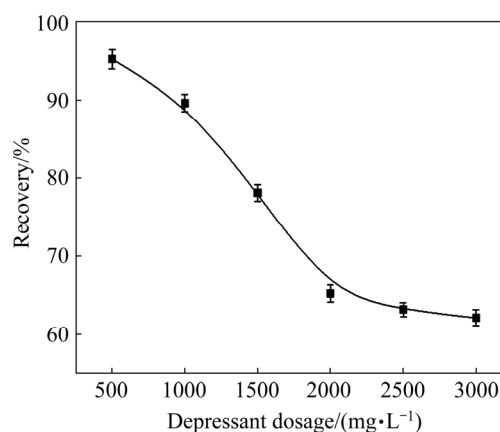

Fig. 4 Flotation performance of covellite as function of depressant dosage (c(ADD)=1×10^{-5} mol/L; mass ratio of NaClO to $FeCl_3$ 4:1; conditioning time of NaClO and $FeCl_3$ 10 and 5 min, respectively; pH=10)
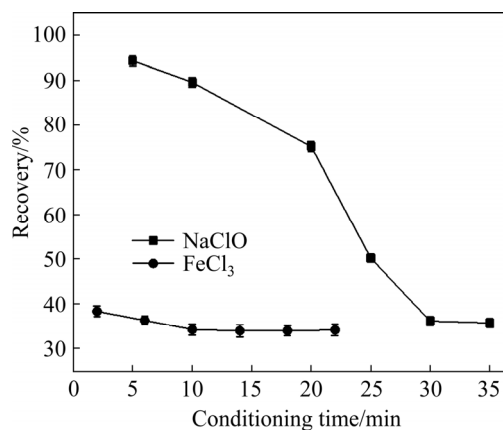

Fig. 5 Flotation performance of covellite as function of depressant conditioning time (c(ADD)=1×10^{-5} mol/L; mass ratio of NaClO to $FeCl_3$ 4:1, pH=10)

results showed that the covellite recovery was mainly affected by the conditioning time of NaClO, and decreased from 94.32% to 36.08% with an increase in the conditioning time from 5 to 30 min, after which it remained constant. By contrast, the impact of the conditioning time of $FeCl_3$ was much smaller than that of NaClO, and the inhibitory effect was the best when the conditioning time was 10 min. Therefore, the conditioning time of the depressants for covellite was much longer than that for other sulfide minerals.

3.2 Depression mechanism of NaClO and $FeCl_3$ depressants

3.2.1 XPS spectra

XPS was used to identify both the chemical compositions and chemical states of the elements on the surfaces of the covellite samples, based on the distinctive binding energies of the inner electrons of each element. XPS is a surface-sensitive technique that can characterize the surface to a depth of less than 10 nm [19,20]. The XPS spectra of the covellite surface before and after treatment with depressants within a binding energy range of 0−1400 eV and atomic concentrations for the covellite surface are shown in Fig. 6.
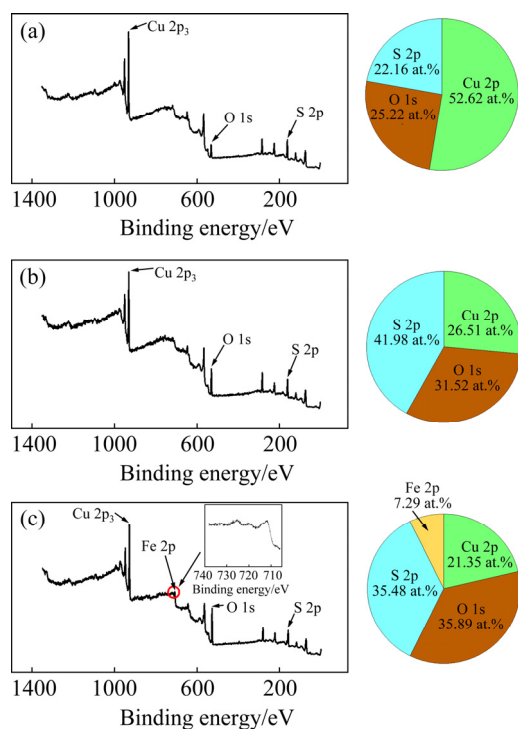

Fig. 6 XPS survey scan results for covellite samples: (a) Fresh covellite; (b) Covellite + NaClO; (c) Covellite + NaClO + $FeCl_3$

As shown in the pie chart in Fig. 6, for the untreated covellite sample, the concentrations of Cu, S, and O were found to be 52.62, 25.22, and 22.16 at.%, respectively, and no Fe was detected. After being treated with NaClO, the Cu concentration decreased to 26.51 at.%, and the O and S concentrations increased to 31.52 and 41.98 at.%, respectively, indicating that the covellite surface was oxidized and Cu(II) was released from the mineral surface to the solution. In the presence of NaClO and $FeCl_3$, the concentrations of Cu, S, and O were 21.35, 35.48, and 35.89 at.%, respectively. Furthermore, the Fe 2p signal was detected, and the concentration of Fe was 7.29 at.%. This revealed that Fe species were adsorbed on the covellite surface, and the covellite surface was further oxidized.

To further investigate the oxidization behavior of covellite, the obtained narrow scan spectra were analyzed using peak fitting, and the relative contents of different compositions were separately determined. The high-resolution XPS spectra for Cu 2p, O 1s, S 2p, and Fe 2p were calculated to obtain the mineral surface atomic chemical states and ratios. The results are shown in Figs. 7−9 and Table 2. These spectra can be used to determine trace amounts of the reaction products on the covellite surface. Semi-quantitative analysis of the atomic concentrations identified the chemical composition of the elements on the mineral surface.

Figure 7 shows the high-resolution XPS spectra of the Cu 2p peaks for the treated and untreated covellite samples. The untreated one (Fig. 7(a)) has two high-intensity peaks at 932.24 and 933.08 eV, representing the binding energies of Cu(I) and Cu(II) in the state of CuS, respectively [21]. Simultaneously, a small peak at 934.96 eV was detected, which was assigned to the CuO or $Cu(OH)_2$ species, indicating that the covellite was slightly oxidized [22]. After treatment with NaClO (Fig. 7(b)), the concentration of the Cu(II)−S species decreased sharply, and the CuO or $Cu(OH)_2$ species increased significantly. In the presence of NaClO and $FeCl_3$ (Fig. 7(c)), this trend was further strengthened, suggesting that the oxidation degree of the covellite sample was slightly increased by $FeCl_3$. The decrease in the active sites of Cu on the covellite surface, which could react with the collector, induced a decrease in its floatability.
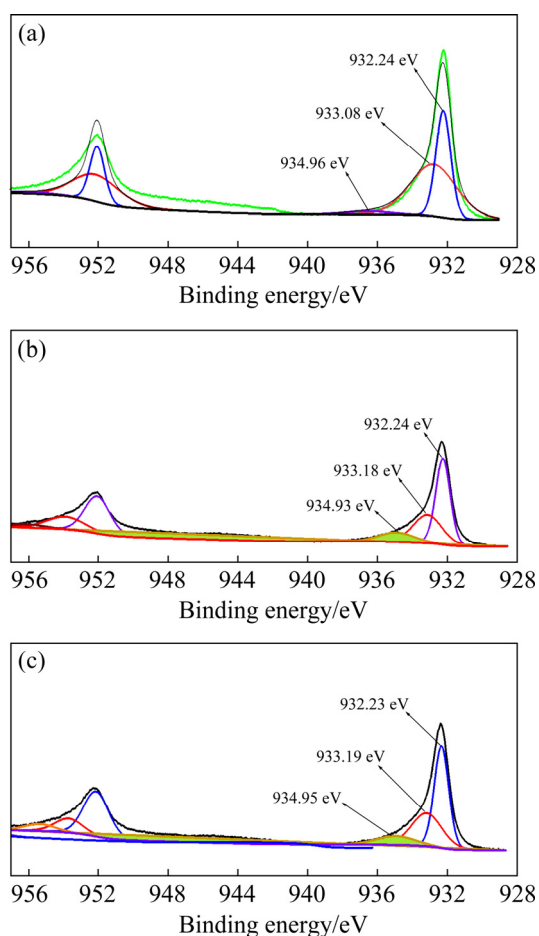
Fig. 7 Cu 2p spectra of covellite samples: (a) Fresh covellite; (b) Covellite + NaClO; (c) Covellite + NaClO + FeCl$_3$

Figure 8 shows O 1s spectra of the covellite samples. As shown in Fig. 8(b), the O 1s spectrum of the covellite sample treated with NaClO fitted reasonably well with three peaks at 532.98, 531.95, and 530.26 eV. The first was assigned to oxygen from carbon–oxygen contaminants [23]. The second was a characteristic of the oxygen in the attached water, and the last was attributed to the oxygen from the oxide species of Cu(II)−O or Cu(II)−OH [24,25]. The amount of O in the form of Cu(II)−O/Cu(II)−OH, as a percentage of the total O, was 13.91 at.%, compared to zero for the fresh covellite. This again showed that the NaClO depressant treatment had a strong oxidation effect on the surface of the covellite. In the presence of FeCl$_3$, the binding energy of the oxidation products changed from 530.26 to 530.91 eV, which may have been due to the formation of the iron hydroxide precipitate, and the value of 530.91 eV was the result of iron oxide and copper oxide [26]. In addition, the proportion of O in the oxide species of Fe(III) or Cu(II) increased from 13.91 to 20.30 at.%, which clearly indicated the formation of the iron hydroxide precipitate on the covellite surface.
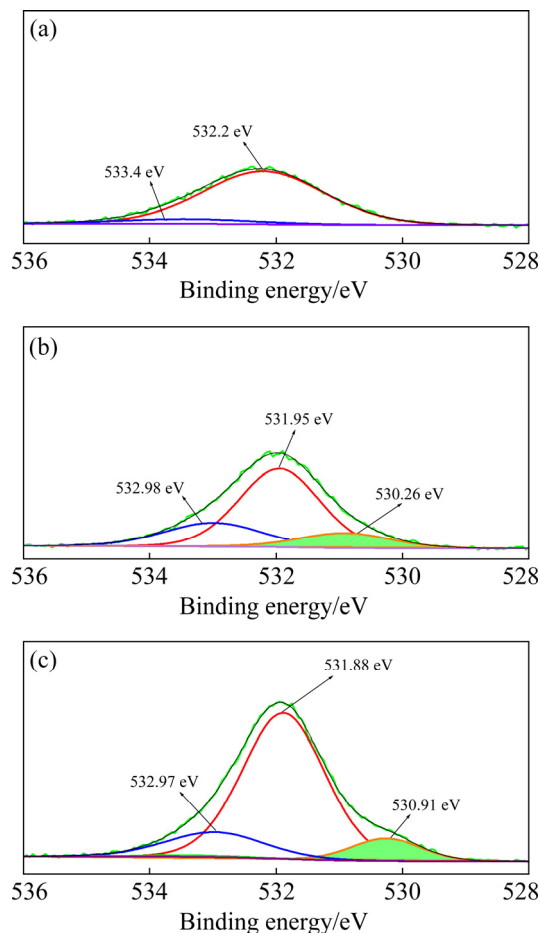

Fig. 8 O 1s spectra of covellite samples: (a) Fresh covellite; (b) Covellite + NaClO; (c) Covellite + NaClO + FeCl$_3$

Figure 9 shows S 2p spectra of covellite samples. Figure 9(b) shows that the S 2p spectra were composed of five pairs of spectral peaks at ~161, ~162, ~163, ~166, and ~168 eV, which correspond to S^{2-}, S_2^{2-}, S_0/S_n^{2-}, SO_3^{2-}, and SO_4^{2-}, respectively [27,28]. S^{2-} and S_2^{2-} exist in covellite, and the other species were identified as products of the oxidation process. After being treated by NaClO, the amount of S in the form of oxidation products, as a percentage of the total S, increased from 36.75 to 47.10 at.%. In the case of the FeCl$_3$ treatment, this proportion was further increased to 55.59 at.%. This indicated that the oxidation process became increasingly intense. The oxidation products of SO_2^{2-} and SO_2^{2-} are hydrophilic substances, which were increased in the presence of the depressants, indicating a decrease in the floatability.
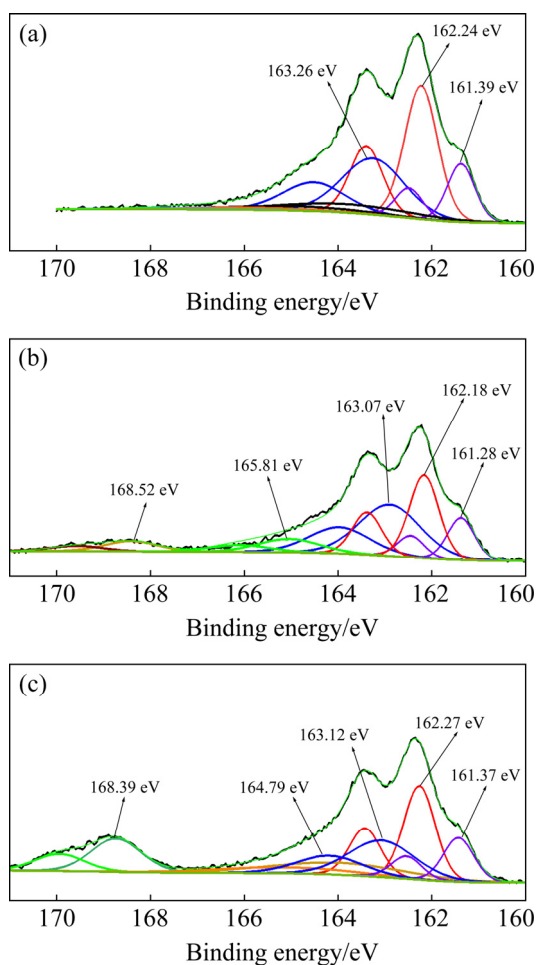
Fig. 9 S 2p spectra of covellite samples: (a) Fresh covellite; (b) Covellite + NaClO; (c) Covellite + NaClO + FeCl$_3$

3.2.2 TOF-SIMS analysis

The compositional changes on the covellite surfaces with or without the depressant treatment were further explored using TOF-SIMS. TOF-SIMS is a sensitive surface analysis technology that can be used to determine the elemental composition and distribution on the surface and body of a sample, and can also provide a secondary ion image of a certain element distribution on the surface [29]. Figure 10 presents digital photographs and peak intensities from positive ion TOF-SIMS analyses of the covellite samples. Ion images of Cu$^+$, CuOH$^+$, and FeOH$^+$ are presented to show their distributions, wherein the bright and dark colors represent regions with higher and lower ion intensities, respectively [30]. For the fresh covellite sample, the image was covered by a bright area, indicating the presence of a large amount of Cu$^+$ on the particle surface. In the presence of NaClO and FeCl$_3$, the image of the covellite sample became dim. There are two possible reasons for this finding. The copper ions on the surface of the mineral could have been released into the solution in an oxidizing environment, or the copper ions on the surface could have been masked by iron hydroxide. As for the distribution of CuOH$^+$, the ion intensity remained almost unchanged after the depressant treatment. As shown in Fig. 10(a), trace amounts of FeOH$^+$ were detected on the untreated covellite

Table 2 Comparison of XPS data for covellite surface with and without depressants

Emission	Species	Untreated		Treated with NaClO		Treated with NaClO and FeCl$_3$	
		BE/eV	RI/%	BE/eV	RI/%	BE/eV	RI/%
	Adsorbed water	533.40	96.51	532.98	23.17	532.97	18.58
O 1s	OH$^-$	532.20	3.49	531.95	62.92	531.88	61.12
	O^{2-}			530.26	13.91	530.91	20.30
	S^{2-}	161.39	16.89	161.28	14.03	161.37	12.54
	S$_2^{2-}$	162.24	46.36	162.18	38.86	162.27	31.87
S 2p	S$_n^{2-}$/S$_0$	163.26	36.75	163.07	30.18	163.07	29.11
	S$_2$O$_3^{2-}$	–	–	165.81	10.14	164.79	16.13
	SO$_4^{2-}$	–	–	168.52	6.78	168.39	10.35
	Cu(I)	932.24	37.46	932.24	54.36	932.23	55.24
Cu 2p	Cu(II)	933.08	58.45	933.18	35.17	933.19	33.57
	Cu(OH)$_2$	934.96	4.10	934.93	10.47	934.95	11.19
Fe 2p	FeOOH	–	–	–	–	713.21	100.00

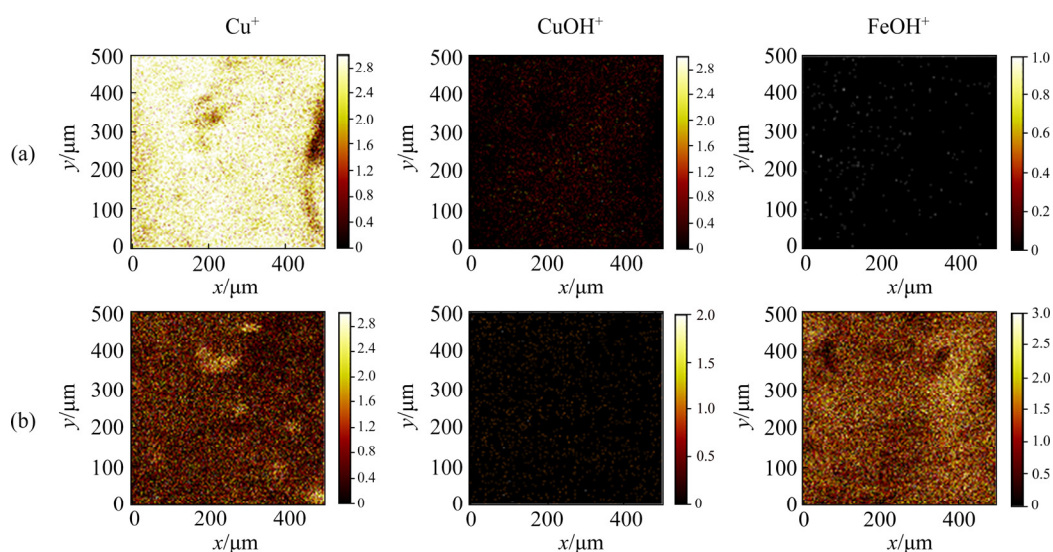BE: Binding energy; RI: Relative intensity

Fig. 10 TOF-SIMS analysis results for covellite treated with and without depressants: (a) Fresh covellite; (b) Covellite + NaClO + FeCl$_3$

surfaces. This could be attributed to impurities in the covellite sample, such as pyrite, which is always associated with covellite. After treatment with NaClO and FeCl$_3$, FeOH$^+$ covered most of the surfaces of the covellite particles with high intensity. The emergence of FeOH$^+$ implied that iron ions covered the mineral surface in the form of iron hydroxide.

The normalized peak intensities were obtained to study changes in the Cu$^+$, CuOH$^+$, and FeOH$^+$ contents. As depicted in Fig. 11, the normalized peak intensity of Cu$^+$ in the fresh covellite was 0.0408, which was much higher than that of the oxidized sample (0.00702). By contrast, the normalized peak intensity of FeOH$^+$ was 0.00927, while there were only trace amounts of FeOH$^+$ on the fresh covellite.
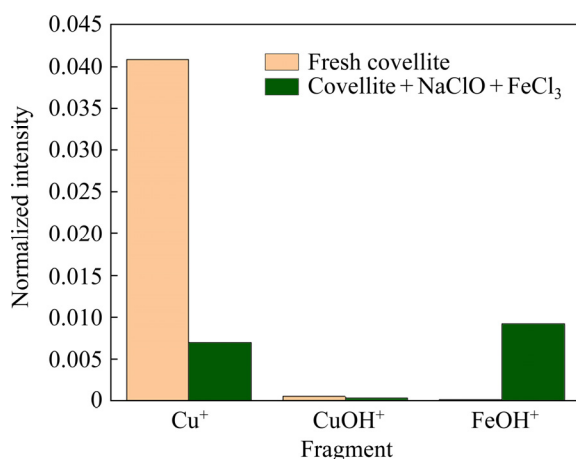

Fig. 11 Normalized intensities of Cu$^+$, CuOH$^+$, and FeOH$^+$ peaks

3.2.3 Contact angle measurements

The changes in the contact angle of a mineral surface before and after treatment with reagents can be used to determine the difference in the hydrophobicity of the mineral. Generally, the surface of a mineral with a small contact angle possesses high hydrophilicity and poor floatability, whereas the surface of a mineral with a large contact angle exhibits good hydrophobicity and floatability [31].

As shown in Fig. 12, the contact angle of the fresh covellite (Sample A) was 30.7°, which is consistent with the results reported by other studies. After treatment with ADD, the contact angle of the covellite (Sample B) increased sharply to 96.7°, indicating that the collector was adsorbed on the mineral surface. The contact angle of Sample C, which was treated with NaClO and then conditioned with ADD, decreased from 96.7° to 80.9°, indicating that the NaClO reduced but did not prevent the adsorption of ADD on the mineral surface. In the presence of FeCl$_3$, the contact angle of the covellite decreased from 80.9 ° to 63.3°, and the hydrophobicity of the surface was greatly reduced. These results are consistent with the results of other studies on floatation.

3.3 Discussion

The oxidization properties of covellite have been widely investigated in the field of hydro-metallurgy [32,33]. Several researchers have proposed a chemical formula for the possible
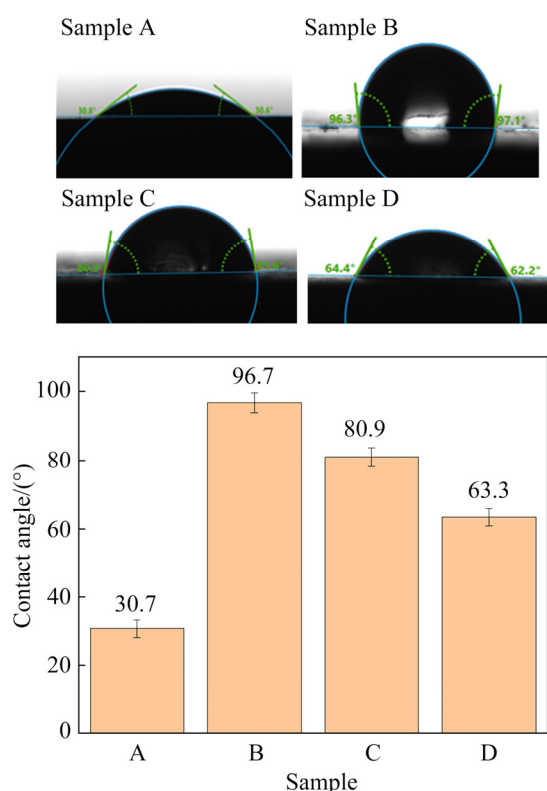
Fig. 12 Contact angle diagrams for four types of covellite samples: Sample A, Fresh covellite; Sample B, Covellite + ADD; Sample C, Covellite + NaClO; Sample D, Covellite + NaClO + FeCl₃

oxidation reaction process of covellite, and they believed that covellite would release copper ions during the oxidation process in an acidic environment and form elemental sulfur and polysulfides on the surface [34]. YIN et al [35] found that, in an alkaline solution, $CuO/Cu(OH)_2$ was generated on the covellite surface. These hydrophilic substances can reduce the floatability of covellites. However, based on the XPS and TOF-SIMS analysis results, little $CuO/Cu(OH)_2$ was generated on the covellite surface, regardless of the depressant treatment. Therefore, most of the $CuO/Cu(OH)_2$ on the covellite dissolved or fell off the mineral surface in the solution. In addition, under the oxidation of NaClO, hydrophobic polysulfide or sulfur species can be generated on the surface of the covellite. These hydrophobic species could increase the floatability of the covellite and counteract the hydrophilic effect of the generated species of $CuO/Cu(OH)_2$. Therefore, NaClO could reduce the active sites of Cu on the covellite surface. However, NaClO alone showed no apparent inhibitory effect on the covellite. FeCl₃ is an oxidant that can form ferric hydroxide colloids in weakly acidic to alkaline environments. This substance was easily adsorbed on the surface and significantly reduced the floatability of the covellite. Meanwhile, the substances that covered the covellite surface hindered the oxidation of sulfide to a certain degree. Under the combined action of NaClO and FeCl₃, the active sites of Cu on the covellite surface were reduced, and the hydrophilic species increased simultaneously, which prevented the adsorption of ADD on the covellite surface. This eventually decreased the floatability of the covellite.

4 Conclusions

(1) Micro-flotation test results indicated that the floatability of covellite could be effectively inhibited by the combined actions of NaClO and FeCl₃. The optimum conditions were pH=10; NaClO and FeCl₃ dosages of 2000 and 500 mg/L, respectively; NaClO and FeCl₃ conditioning time of 30 and 10 min, respectively.

(2) Based on XPS and TOF-SIMS analyses, the depressing effect of NaClO on the covellite was due to the formation of oxidation products on the covellite surface, including CuO and $Cu(OH)_2$, as well as a decrease in the number of Cu active sites. The depressing effect of FeCl₃ was attributed to the precipitation of iron hydroxide on the covellite surface.

(3) Contact angle measurements indicated that Cu/Fe oxides or hydroxides on the surface of the covellite could reduce the adsorption of collectors on the surface, thereby reducing the floatability of the covellite.

References

[1] PÉREZ K, TORO N, SALDAÑA M, SALINAS-RODRÍGUEZ E, ROBLES P, TORRES D, JELDRES R I. Statistical study for leaching of covellite in a chloride media [J]. Metals, 2020, 10: 477.

[2] LUNDSTRÖM M, LIIPO J, TASKINEN P, AROMAA J. Copper precipitation during leaching of various copper sulfide concentrates with cupric chloride in acidic

solutions [J]. Hydrometallurgy, 2016, 166: 136−142.

[3]   LIU H C, XIA J L, NIE Z Y, WEN W, YANG Y, MA C Y, ZHENG L, ZHAO Y D. Formation and evolution of secondary minerals during bioleaching of chalcopyrite by thermoacidophilic archaea acidianus manzaensis [J]. Transactions of Nonferrous Metals Society of China, 2016, 26: 2485−2494.

[4]   YIN W Z, YANG B, FU Y F, CHU F D, YAO J, CAO S H, ZHU Z L. Effect of calcium hypochlorite on flotation separation of covellite and pyrite [J]. Powder Technology, 2019, 343: 578−585.

[5]   CHANDRA A P, GERSON A R. A review of the fundamental studies of the copper activation mechanisms for selective flotation of the sulfide minerals, sphalerite and pyrite [J]. Advances in Colloid and Interface Science, 2009, 145: 97−110.

[6]   PLACKOWSKI C, NGUYEN A V, BRUCKARD W J. A critical review of surface properties and selective flotation of enargite in sulphide systems [J]. Minerals Engineering, 2012, 30: 1−11.

[7]   TAYEBI-KHORAMI M, MANLAPIG E, FORBES E, BRADSHAW D, EDRAKI M. Selective flotation of enargite from copper sulphides in Tampakan deposit [J]. Minerals Engineering, 2008, 112: 1−10.

[8]   SMITH L K, BRUCKARD W J. The separation of arsenic from copper in a Northparkes copper−gold ore using controlled-potential flotation [J]. International Journal of Mineral Processing, 2007, 84: 15−24.

[9]   FORNASIERO D, FULLSTON D, LI C, RALSTON J. Separation of enargite and tennantite from non-arsenic copper sulfide minerals by selective oxidation or dissolution [J]. International Journal of Mineral Processing, 2001, 61: 109−119.

[10] TAYEBI-KHORAMI M, MANLAPIG E, FORBES E, EDRAKI M, BRADSHAW D. Effect of surface oxidation on the flotation response of enargite in a complex ore system [J]. Minerals Engineering, 2018, 119: 149−155.

[11] SENIOR G D, GUY P J, BRUCKARD W J. The selective flotation of enargite from other copper minerals—A single mineral study in relation to beneficiation of the Tampakan deposit in the Philippines [J]. International Journal of Mineral Processing, 2006, 81: 15−26.

[12] BRUCKARD W J, KYRIAKIDIS I, WOODCOCK J T. The flotation of metallic arsenic as a function of pH and pulp potential—A single mineral study [J]. International Journal of Mineral Processing, 2007, 84: 25−32.

[13] FILIPPOU D, ST-GERMAIN P, GRAMMATIKOPOULOS T. Recovery of metal values from copper−arsenic minerals and other related resources [J]. Mineral Processing and Extractive Metallurgy Review, 2007, 28: 247−298.

[14] GUL A, BULUT G, SIRKECI A A. Beneficiation of arsenic-bearing complex sulphide ore by flotation [J]. Physicochemical Problems of Mineral Processing, 2013, 49: 203−212.

[15] HAGA K, TONGAMP W, SHIBAYAMA A. Investigation of flotation parameters for copper recovery from enargite and chalcopyrite mixed ore [J]. Materials Transactions, 2012, 53: 707−715.

[16] DENG R D, HU Y, KU J G, ZUO W R, YANG Z G.

Adsorption of Fe(III) on smithsonite surfaces and implications for flotation [J]. Colloids and Surfaces A: Physicochemical and Engineering Aspects, 2017, 533: 308−315.

[17] DENG R D, YANG X F, HU Y, KU J G, ZUO W R, MA Y Q. Effect of Fe(II) as assistant depressant on flotation separation of scheelite from calcite [J]. Minerals Engineering, 2018, 118: 133−140.

[18] LI Y Q, CHEN J H, KANG D, GUO J. Depression of pyrite in alkaline medium and its subsequent activation by copper [J]. Minerals Engineering, 2012, 26: 64−69.

[19] NOWAK P, LAAJALEHTO K. Oxidation of galena surface: An XPS study of the formation of sulfoxy species [J]. Applied Surface Science, 2000, 157: 101−111.

[20] WU D D, WEN S M, DENG J S, LIU J, MAO Y B. Study on the sulfidation behavior of smithsonite [J]. Applied Surface Science, 2015, 329: 315−320.

[21] CAPECE F M, CASTRO V D, FURLANI C, MATTOGNO G, FRAGALE C, GARGANO M, ROSSI M. "Copper chromite" catalysts: XPS structure elucidation and correlation with catalytic activity [J]. Journal of Electron Spectroscopy and Related Phenomena, 1982, 27: 119−128.

[22] HIRAJIMA T, MIKI H, SUYANTARA G P W, MATSUOKA H, ELMAHDY A M, SASAKI K, IMAIZUMI Y, KUROIWA S. Selective flotation of chalcopyrite and molybdenite with H_2O_2 oxidation [J]. Minerals Engineering, 2017, 100: 83−92.

[23] MCINTYRE N S, ZETARUK D G. X-ray photoelectron spectroscopic studies of iron oxides [J]. Analytical Chemistry, 1977, 49: 1521−1529.

[24] XIONG X L, HUA X M, ZHENG Y F, LU X G, LI S G, CHENG H W, XU Q. Oxidation mechanism of chalcopyrite revealed by X-ray photoelectron spectroscopy and first principles studies [J]. Applied Surface Science, 2018, 427: 233−241.

[25] TAN B J, KLABUNDE K J, SHERWOOD P M A. X-ray photoelectron spectroscopy studies of solvated metal atom dispersed catalysts: Monometallic iron and bimetallic iron−cobalt particles on alumina [J]. Chemistry of Materials, 1990, 2: 186−191.

[26] HUA X M, ZHENG Y F, XU Q, LU X G, CHENG H W, ZOU X L, SONG Q S, NING Z Q. Interfacial reactions of chalcopyrite in ammonia−ammonium chloride solution [J]. Transactions of Nonferrous Metals Society of China, 2018, 28: 556−566.

[27] NESBITT H W, MUIR I J, PRARR A R. Oxidation of arsenopyrite by air and air-saturated, distilled water, and implications for mechanism of oxidation [J]. Geochimica et Cosmochimica Acta, 1995, 59: 1773−1786.

[28] IRANMAHBOOB J, GARDNER S D, TOGHIANI H, HILL D O. XPS study of molybdenum sulfide catalyst exposed to CO and H_2 [J]. Journal of Colloid and Interface Science, 2004, 270: 123−126.

[29] LAI H, DENG J S, WEN S M. Application of ToF-SIMS and PCA to study interaction mechanism of dodecylamine and smithsonite [J]. Applied Surface Science, 2019, 496: 143698.

[30] LIU R Z, LIU D W, LI J L, LIU S Y, LIU Z C, GAO L Q, JIA X D, AO S F. Improved understanding of the sulfidization mechanism in cerussite flotation: An XPS, ToF-SIMS and FESEM investigation [J]. Colloids and

Surfaces A: Physicochemical and Engineering Aspects, 2020, 595: 124508.

[31] HOLUSZKO M E, FRANZIDIS J P, MANLAPIG E V, HAMPTON M A, DONOSE B C, NGUYEN A V. The effect of surface treatment and slime coatings on ZnS hydrophobicity [J]. Minerals Engineering, 2008, 21: 958−966.

[32] DUTRIZAC J E, MACDONALD R J C. Ferric ion as a leaching medium [J]. Minerals Science and Engineering, 1974, 6: 59−100.

[33] MIKI H, NICOL M, VELÁSQUEZ-YÉVENES L. The

kinetics of dissolution of synthetic covellite, chalcocite and digenite in dilute chloride solutions at ambient temperatures [J]. Hydrometallurgy, 2011, 105: 321−327.

[34] NICOL M J, TJANDRAWAN V, ZHANG S C. Cathodic reduction of iron(III) and copper(II) on various sulfide minerals in chloride solutions [J]. Hydrometallurgy, 2016, 166: 113−122.

[35] YIN Q, VAUGHAN D J, ENGLAND K E R, KELSALL G H. Electrochemical oxidation of covellite (CuS) in alkaline solution [J]. Journal of Colloid and Interface Science, 1994, 166: 133−142.

氧化环境下铜蓝的表面性质、捕收剂吸附和浮选特性

甘永刚 [1,2,3]，邓荣东 [4]，刘全军 [1]

1. 昆明理工大学 国土资源工程学院，昆明 650093；
2. Serbia Zijin Mining Doo Bor, Bor 19210, Serbia;
3. 紫金矿业集团股份有限公司，龙岩 364200；
4. 福州大学 紫金矿业学院，福州 350108

摘　要：采用微型浮选试验、X 射线光电子能谱(XPS)、飞行时间二次离子质谱(TOF-SIMS)和接触角测量技术对铜蓝在 NaClO 和 FeCl₃作用下的表面特征、捕收剂吸附和浮选特性进行研究。微型浮选试验结果表明，NaClO 和 FeCl₃的存在能有效抑制铜蓝，但所需抑制剂的用量大，且调浆时间长。XPS 和 TOF-SIMS 分析结果表明，NaClO 能氧化铜蓝表面，减少 Cu 的活性位点，并在铜蓝表面生成 CuO 和 Cu(OH)₂等氧化产物。添加 FeCl₃后，氢氧化铁在铜蓝表面的沉淀使矿物表面亲水物质的含量增加，阻止丁铵黑药在铜蓝表面的吸附，从而使铜蓝可浮性进一步降低。

关键词：铜蓝；可浮性；飞行时间二次离子质谱(TOF-SIMS)；NaClO；FeCl₃

(Edited by Wei-ping CHEN)